



Missouri University of Science and Technology
Scholars' Mine

International Conference on Case Histories in Geotechnical Engineering (2008) - Sixth International Conference on Case Histories in Geotechnical Engineering

14 Aug 2008, 2:20 pm - 2:30 pm

Cratering and Blowing Soil by Rocket Engines During Lunar Landings

Philip T. Metzger

NASA, KT-D3, Kennedy Space Center, FL

John E. Lane

ASRC Aerospace, Kennedy Space Center, FL

Christopher D. Immer

ASRC Aerospace, Kennedy Space Center, FL

Sandra Clements

ASRC Aerospace, Kennedy Space Center, FL

Follow this and additional works at: <https://scholarsmine.mst.edu/icchge>

 Part of the [Geotechnical Engineering Commons](#)

Recommended Citation

Metzger, Philip T.; Lane, John E.; Immer, Christopher D.; and Clements, Sandra, "Cratering and Blowing Soil by Rocket Engines During Lunar Landings" (2008). *International Conference on Case Histories in Geotechnical Engineering*. 1.

<https://scholarsmine.mst.edu/icchge/6icchge/session10/1>

This Article - Conference proceedings is brought to you for free and open access by Scholars' Mine. It has been accepted for inclusion in International Conference on Case Histories in Geotechnical Engineering by an authorized administrator of Scholars' Mine. This work is protected by U. S. Copyright Law. Unauthorized use including reproduction for redistribution requires the permission of the copyright holder. For more information, please contact scholarsmine@mst.edu.



CRATERING AND BLOWING SOIL BY ROCKET ENGINES DURING LUNAR LANDINGS

Philip T. Metzger

NASA, KT-D3

Kennedy Space Center, FL-USA 32899

John E. Lane

ASRC Aerospace

Kennedy Space Center, FL-USA 32899

Christopher D. Immer

ASRC Aerospace

Kennedy Space Center, FL-USA 32899

Sandra Clements

ASRC Aerospace

Kennedy Space Center, FL-USA 32899

ABSTRACT

This paper is a summary compilation of work accomplished over the past decade at NASA's Kennedy Space Center to understand the interactions between rocket exhaust gases and the soil of the Moon or Mars. This research is applied to a case study of the Apollo 12 landing, in which the blowing soil peppered the nearby Surveyor III spacecraft producing measurable surface damage, and to the Apollo 15 landing, in which the Lunar Module tilted backwards after landing in a crater that was obscured from sight by the blowing dust. The modeling coupled with empirical observations is generally adequate to predict the order of magnitude of effects in future lunar missions and to formulate a rough concept for mitigating the spray around a lunar base. However, there are many significant gaps in our understanding of the physics and more effort is needed to understand the problem of blowing soil so that specific technologies can be developed to support the lunar outpost.

INTRODUCTION

Without proper controls, the high temperature, supersonic jet of gas that is exhausted from a rocket engine is capable of damaging both the rocket itself and hardware in the surrounding environment. For about seven decades, NASA has invested significant effort into understanding and controlling these effects at the terrestrial launch pads [Schmalzer et al, 1998], and while the efforts have been largely successful, some damage to surrounding hardware still occurs on a routine basis. These challenges also exist when launching or landing rockets on other planetary bodies, such as the Moon, Mars, or asteroids. The exhaust gases of the landing or launching spacecraft could kick up rocks, gravel, soil, and dust. This can cause damage to the landing spacecraft or to other hardware that has already been landed in the vicinity. It can also spoof the sensors of the landing spacecraft and block visibility of natural terrain hazards, resulting in significant risk of an unsuccessful landing.

To date, humans have completed only 22 successful retro-rocket landings on other bodies. The United States landings included five robotic missions on the Moon in the Surveyor program, six human-piloted missions on the Moon in the Apollo program, two robotic missions on Mars in the Viking program, and one robotic mission on the asteroid Eros. At the time that this paper was written, the Phoenix mission was en-route for a retro-rocket

landing on Mars. The successful Russian landings with retro-rockets have included seven robotic missions on the Moon in the Luna program and one robotic mission in the Mars program. Closely related to these, there were twelve terrestrial launches and landings of the DC-X rocket on the packed gypsum-powder surface of White Sands, New Mexico. The last of these missions resulted in the loss of the vehicle at landing, but not because of exhaust plume interactions. (The U.S. program has also landed three spacecraft on Mars using airbags rather than rockets at touchdown; the Russian program has landed ten spacecraft on Venus using parachutes and aerobraking; and the European program has landed one spacecraft on Saturn's moon Titan using a parachute.) There have been quite a few unsuccessful attempts to land with retro-rockets on other bodies, but so far none of these failures have been attributed to the exhaust plume's interaction with the surface

In the upcoming U.S. return to the Moon, there will be a greater concern with plume/soil interactions than in prior missions. That is because the landers will be larger with more thrust and because spacecraft will land and launch repeatedly in the vicinity of the lunar outpost, subjecting the hardware assets on the Moon to repeated high-velocity spraying of dust, soil, and possibly larger ejecta. Fortunately, there have been several cases of prior landings that provide significant insight into the possible effects of this spraying material. This paper analyzes the Apollo 12 and

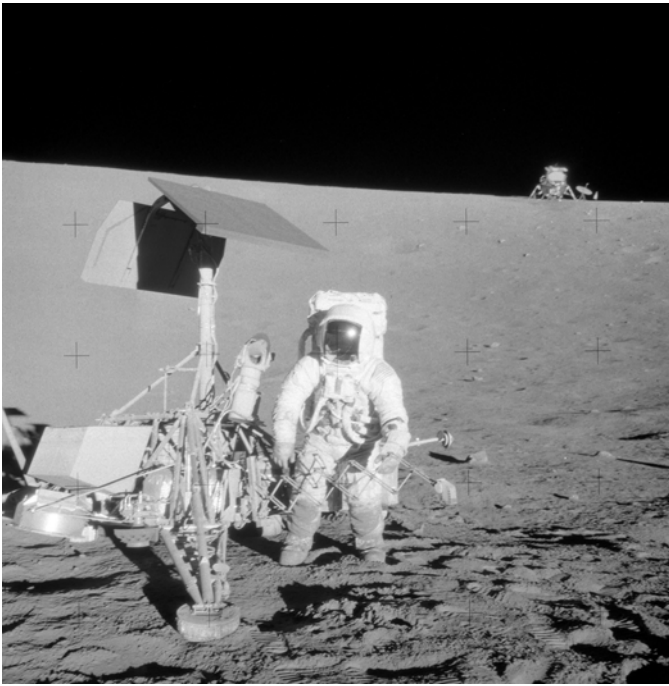


Fig 1. Pete Conrad at Surveyor III with Apollo 12 LM in background

Apollo 15 landings as case studies in comparison with recent experiments and analysis.

THE PROBLEM

The Apollo 12 Lunar Module (LM) landed less than 200 meters away from the Surveyor III spacecraft as shown in Fig. 1. At the time, this distance was thought to be sufficient to minimize the effects that blowing soil might have upon the Surveyor spacecraft. The astronauts walked to the Surveyor, inspected it and removed portions for analysis on Earth in order to learn how the materials had been affected by the space environment (cosmic rays, micrometeoroids, vacuum, etc.). An interesting feature of the Surveyor hardware is that it had been sandblasted by a high-speed shower of sand and dust particles during the LM's landing [Jaffe, 1972]. The sandblasting cast permanent "shadows" onto the materials, and these shadows were mathematically triangulated to a location on the lunar surface directly beneath the engine of the landed LM. Judging by the sharpness of the shadows and the lack of curvature allowable for the particles to fit the trajectory, investigators concluded that the particles must have been moving in excess of 100 m/s. Additional to this general scouring of the surface, there were discrete micro-crates or divots peppering its surface. Presumably the overall scouring was due to the large number of dust particles while the divots were due to the much smaller number of larger soil particles. Brownlee et al [1972] studied the morphology of the resulting microscopic divots on the Surveyor's camera glass and estimated the particle were traveling between 300 and 2000 m/s. The authors have roughly estimated from the published reports and from the several boxes of engineering logbooks and documents at the lunar curation building at NASA's Johnson



Fig. 2. Apollo 15 LM tilted backwards 11 degrees into a shallow crater.

Space Center that there were on the order of 1.4 divots/cm² on the side of the Surveyor camera cover facing the LM. Also, the Surveyor hardware had been injected by dust and sand particles that were blown into the tiny crevices and openings [Benson et al, 1972].

During the Apollo 15 landing, the crew reported that the blowing dust was visible from 46 m altitude and that from 18 m down the blanket of dust blowing across the field of view became so opaque that the landing had to be accomplished with zero visibility of the surface [Mitchell et al, 1972a]. On the other Apollo landings the visibility was not as bad [Mitchell et al, 1972b, Mitchell et al, 1973]. At footpad contact the LM rocked backward approximately 11 degrees from vertical before coming to rest [McDivitt et al, 1971], as shown in Fig. 2. One of the astronauts exclaimed "bam" over the radio coincident with the second contact event that terminated the backward rocking motion. It turns out that the LM had landed on the rim of a broad, shallow crater with two of its legs suspended in space over the crater and the other two legs resting on the soil outside the crater. It rocked backwards and to the left into the crater until three of the four legs were making contact with the soil, with the remaining leg of the LM (the front leg, which was outside the crater) bearing no weight. The crater had not been visible to the astronauts during landing in part because it was shallow and hence inadequately shadowed in the center, and in part because the dense blanket of dust that was blowing over obscured it as illustrated by Fig. 3. As a result, the crew was not able to steer the LM past the crater to avoid the landing hazard. The resulting tilt angle of the LM was not so severe that it prevented successful completion of the mission, but it illustrates the potential problem of terrain features hidden by the dust.

The Apollo 12 experience illustrates that blowing material can damage nearby hardware. The Apollo 15 experience illustrates that it can pose a hazard to the lander, itself. In the context of the very successful Apollo program, these two situations were minor considerations to the respective missions and should not be exaggerated. In the context of returning to the Moon with multiple landings in the vicinity of a lunar outpost, they serve very usefully as case studies of the plume-soil interactions. From these measured effects, it is possible to calibrate a model of blowing soil and to gauge how much damage will be caused by future rockets as they launch and land in the vicinity of other hardware on the Moon.



Figure 3. View from Apollo 15 LM descent imager camera, with distorted shadow of LM leg, footpad and soil contact probe draped across the blowing dust cloud (from the top center of the figure and pointing downward). Surface terrain features are not visible beneath the blowing dust.

To quantify the damage that may occur to surrounding hardware, it is crucial to quantify the erosion rate and total quantity of ejected soil. The estimates from the Apollo program did not agree with one another. One method to estimate the erosion rate was to first perform small scale experiments in vacuum chambers and measure the erosion rate [Clark and Land, 1963; Land and Clark, 1965; Land and Conner, 1967; Land and Scholl, 1969]. Then, Mason and Nordmeyer [1969] derived an empirical law for the erosion rate based upon these experiments, but calibrating the unknown effects of the lunar environment by the volume of the putative crater formed under the nozzle of vernier engine number three on the Surveyor V spacecraft, as seen in photographic images taken by that spacecraft. Mason [1970] used this erosion rate with the actual descent trajectory of the Apollo 11 spacecraft to calculate the expected soil erosion beneath the LM, and estimated that the crater depth would be in the range 1.3 – 2.0 cm (reported as 0.5 – 0.8 in.) and that the eroded volume would be in the range 36 – 57 liters (reported as 2200 – 3500 cu in.). A vastly higher erosion volume was estimated by R. F. Scott [1975] for Apollo 12 based on the number of particles required per square centimeter to scrub permanent shadows into the surface of the Surveyor III. Based on a several assumptions, Scott estimated a removed soil depth of 18 – 25 cm (reported as 7 – 10 in.) over a radius of 2.3 m (reported as a diameter of 15 feet). The details of the calculation are not provided, but if he had assumed a conical crater shape, then this would represent a total eroded volume of 973 – 1390 liters, and if a cylindrical crater shape then this would represent 1460 – 2080 liters. A sphere-section crater shape would be intermediate to the cone and cylinder. Scott's smallest possible estimate of total erosion volume was 57 times greater than Mason's largest estimate. This cannot be attributed merely to differences in the landing zone soils or the trajectories of the two missions, so we must conclude that one or both estimates are not accurate. In both cases, the depth of soil removal was small compared to the natural terrain variations so that it would not be possible to identify a broadly

tapering crater superimposed upon that terrain. Thus, it is not possible to directly measure its volume for any particular mission. Another comparison comes from Apollo 14 where a distinct, localized erosion crater was found near the nozzle of the landed LM, but it was probably due to a localized enhancement of the erosion rate where the LM's soil contact probe had penetrated and broken up the hard-packed surface. The volume of that localized crater was estimated to be 440 liters [Katzan and Edwards, 1991], and does not include any eroded soil over the broader region around the LM, so it does not provide an estimate of the natural erosion rate apart from the mechanical disturbance of the contact probe in this one case.

Another critical parameter to quantify is the ejection angle of the soil, because this will determine whether the soil will miss the surrounding hardware by flying over it or whether the soil can be blocked with a modest berm built by piling lunar soil around the landing zone. There was no clear consensus in the prior literature as to what determines the ejection angle. Roberts [1963a; 1963b; 1964; 1966] had assumed that aerodynamic forces do not significantly affect the ejection angle, so that the soil is ejected at the same angle as the local terrain slope, which acts as a ballistic ramp. Thus, the large and small particles will all be ejected into the same angle. However, we have observed in the Apollo videos that the dust blowing out from meter-scale impact craters on the lunar surface are ejected at an angle that modulates up or down coincident with the LM increasing and decreasing its thrust, and this indicates that the aerodynamics are a controlling factor and cannot be neglected. The scaled experiments discussed above did not measure ejection angles. A report on the conceptual design of a lunar base [Phillips et al, 1988; Phillips et al, 1992] used a plume flowfield calculated for free space [Alred, 1983], ignoring the presence of the lunar surface. This method ignores the all-important horizontal flow that develops across the lunar surface beneath the standoff shockwave and therefore cannot produce correct results.

This brief review indicates that neither the mass erosion rate nor the ejection angles have been adequately determined. The following sections of this paper describe additional methods to constrain these parameters.

THEORETICAL BACKGROUND

Prior to each of the Surveyor, Apollo and Viking programs, NASA undertook a series of investigations to understand and quantify some of these physical phenomena to help ensure mission success. These studies discovered that the gas-soil erosion processes under a supersonic jet can be a complex set of solid/fluid interactions, depending upon the specific conditions of the jet and soil. To this day parts of the physics have not been accurately described or explained. Even a very basic, qualitative physical explanation has been lacking until recently for some aspects of a jet-induced cratering event. During the Apollo and Viking missions it was not necessary to fully understand these phenomena because the spacecraft engines were designed to prevent the most energetic of these processes from occurring. That is, the pressure developed upon the Lunar or Martian regoliths in the stagnation region of the impinging jets was kept

sufficiently low to prevent the bearing capacity failure of the soil which otherwise may have occurred. This was possible in the lunar landings because the small mass of the LMs and the weak lunar gravity made it possible to use a lower thrust and because the unweathered lunar soil is very compacted with extremely high shear strength and very low gas permeability [Carrier et al, 1991]. However, the lunar regolith has a very loose layer of surface material (dust and sand-sized particles), just a few centimeters thick, and so the surface erosion of this loose material appears to be the primary effect in these landings.

Roberts [1963a; 1963b; 1964; 1966] developed a theory of this *viscous erosion* (VE) mechanism for lunar dust. His method was adopted by J. S. Dohnanyi [1966] to apply to the design of the LM engines. Roberts derived a set of equations which calculate the shear stresses on a flat, dust-covered surface, and calculated the quantity of material which would be entrained into the gas flow as a function of radial distance from the center of the plume. The region of maximum shear stress turned out to be a ring some distance out from the center of the exhaust because the gas velocity (v) increases radially while its density (ρ) decreases into the lunar vacuum and thus the dynamic pressure ($\rho v^2/2$) is a maximum at some finite radius. Hutton [1968] compared the theory to the small-scale experiments in vacuum chambers by Clark et al, cited above, and found only limited correlation. We believe that this is partly because of the simplifications in Roberts' theory, but also partly because the experiments did not adequately simulate the lunar conditions. For example, Roberts' erosion rate equation omits the effect of particles eroded upstream in the flow upon the erosion rate of soil downstream in the flow. This is a good approximation only when the erosion processes occur over a small distance relative to the length scale of the flow field, but in the small scale experiments the flow field is very small and so this approximation is not appropriate. Furthermore, the volumetric erosion rate was so high in the experiments compared to the lunar case that the shape of the surface changed dramatically during the test, whereas Roberts assumed a flat surface.

Few studies have been done on the other exhaust cratering mechanisms besides VE. One such experimental study was performed by Alexander et al [1966]. This study discussed VE but focused primarily upon *bearing capacity failure* (BCF) as a cratering mechanism, in that the stagnation pressure of gas directly beneath a jet may exceed the bearing capacity of the soil and mechanically push it downward, forming a crater under the jet. Cold gas jets and hot engine firings were used to create craters in sand and clay, and the resulting craters were measured for various dimensions. The data were compared to identify significant parameters and scaling relationships. The authors developed several methods to predict the approximate crater dimensions, including (1) an analogy to the classic cone penetrator test, (2) a refinement of the cone penetration model in which the diffusion of gas into the soil is assumed to have reached steady state to weaken the soil according to Terzaghi's effective stress hypothesis, (3) a purely elastic model of the sand to provide an order-of-magnitude estimate of the width of sand that would fail and be removed in the initial crater formation, and (4) a yield-strength analysis using the equations of soil

mechanics to calculate the stresses as a function of distance beneath a point load to estimate crater depth. The experimental methods did not provide a direct view beneath the surface during or after the BCF event, so the major features of these models were untested.

Another study in this Apollo era by Scott and Ko [1968] identified the *diffused gas eruption* (DGE) mechanism. Whereas Alexander et al were concerned only with how gas diffusion enhanced the BCF mechanism, Scott and Ko treated the gas diffusion as a distinct soil-moving mechanism in its own right. They fired rocket motors into soil and observed the results with a high-speed video camera. They discovered that radial diffusion of pressure could eventually blow out a toroidal region around the exhaust jet. This occurred because the high pressure gas diffusing into the soil beneath the engine would diffuse radially outwardly from the jet until the pressure of gas beneath the surface at some radial distance was sufficient to lift the overlying column of soil. They also found that when the rocket was shut off a spike of soil could blow up the center of the rocket nozzle as the gases quickly diffused back out from the soil. The investigators modeled these effects with a numerical, finite-difference algorithm. The model successfully predicted the DGE in the toroidal region during jet firing and also in the central region after jet cutoff. Hon-Yim Ko [1971] provided an improved analysis of how gas diffusion enhances BCF. That paper is presently inaccessible to the authors. Apparently, it describes a finite element program to analyze both gas diffusion and BCF, but the program did not produce sufficiently accurate results due to the limited computing capabilities available at the time.

During the lead-up to the Viking landings on Mars, a series of papers were authored with the interest in avoiding BCF altogether and keeping DGE to levels that could be safely ignored. In contrast to the lunar case, the thin Martian atmosphere will collimate rocket exhausts [Foreman, 1967] and focus the stagnation pressure onto a small portion of the regolith. Roberts' model therefore needed to be modified before it could be applied to Mars. Clark [1970] tested a scaled Viking lander in a 60-foot vacuum sphere, paying special attention to the cant angle of the nozzles on the multi-engine lander. Another Viking study [Romine et al 1973] addressed exhaust cratering both theoretically and experimentally, showing that a conventional bell nozzle would affect the surface too much beneath the lander and making a number of significant contributions to our understanding of the physics. Finally, Hutton et al [1980] described the observed disturbances that were actually caused by the Viking retro-rockets landing on Mars. These Mars studies provide some physical intuition of the physics for the lunar case, but cannot be directly applied to it due to the environmental differences.

To summarize, the investigations supporting the Apollo and Viking programs determined that there are several physical mechanisms of interaction between gas jets and soil. The identified mechanisms were viscous erosion (VE), diffused gas eruption (DGE), and bearing capacity failure (BCF). These will occur in varying proportions depending upon the particular

conditions of the soil and the jet. Roberts' theory assumed implicitly that VE is the only mechanism capable of moving soil during the lunar landing. Experience shows that bearing capacity failure did not occur under the exhaust plumes in the Apollo program. Probably the bearing capacity of the lunar soil was sufficient to resist cratering because of its very high internal friction and its relatively low gas permeability. The area under the nozzle in each mission had a "swept clean" appearance as shown in Fig. 4, missing the loose layer of un-compacted soil and dust that was characteristic everywhere else on the Moon.



Fig. 4. Area under Apollo 12 LM engine nozzle showing how surface has been "swept clean" of loose material. The narrow trench in the upper left part of picture was dug by the soil contact probe as it dragged beneath the descending LM.

Because the soil around the nozzle was so undisturbed, it is unlikely that any DGE occurred after engine cutoff. On the landing videos, a thin, dusty mist is visible for a few seconds after engine cutoff, and this probably represents the entrainment of only very tiny dust particles as the regolith depressurizes. In light of these things, it would seem that the looser surface soil was swept away from beneath the nozzle but the deeper, more compacted layers remained in place. Nevertheless, it is problematic to explain this by Roberts' theory, because the shear stress of the gas is zero at the stagnation point under the center of the nozzle, and very low for a significant radius around that point until at higher distances the gas velocity becomes sufficiently high to move the soil. So what sweeps the soil away from the centerline of a jet? Similarly, in loose sand, why is a jet-induced crater deepest in the center where the gas velocity is zero? A simple test can show that a jet easily forms a crater even when its dynamic pressure is far below the pressure that the sand can support, and so BCF must not be the general explanation for the motion of sand directly under a jet. This is relevant to predicting the erosion rate of the Apollo missions since the combination of

mechanisms that move the soil may predict a different rate than Roberts' theory, which assumes the mechanism to be VE, alone.

EXPERIMENTS OF CRATERING MECHANISMS

To gain more insight into the physics, tests were performed at ambient pressure with sand impinged normally by jets composed of different gases (nitrogen, carbon dioxide, argon and helium) to provide variations in gas density. The tests were performed with different exit velocities, different nozzle heights above the sand, and with different sized sand grains. The tests used two methods to identify soil behavior beneath the surface. In the first method, a sandbox was prepared with horizontal layers of different colored sand. A vertical jet was impinged upon the sandbox forming a vertical burst of sand that left a shallow, residual crater on the surface. This was filled in with black sand so that the crater would not slump while filling with epoxy and to provide color contrast as a record of the crater shape. Optically clear epoxy was diffused into the pore spaces of the sand and thermally cured so that it could be cut in half to reveal the deformation of the layers beneath the surface. The prediction from the model of Alexander, *et al.*, was that the layers would be bent downward beneath the crater as they would be due to cone penetration. However, we found that the sand was pulled upward along the crater axis as shown in Fig. 5, quite the opposite of what we expected.



Fig. 5. Cutaway view of sand layers (originally horizontal) as they were deformed beneath the surface of a crater.

To explain this subsurface flow, the second test method performed the cratering on the edge of the sandbox with a clear window to see into the subsurface during the test. The top edge of the box was beveled outwardly to bisect the jet with minimal disturbance of the flow inside the sand, as shown in Figure 6. Two regimes of gas-sand interaction were observed as a function of jet velocity. For the higher velocity (but still subsonic) regime, the cratering was seen to consist of a very deep, very narrow, cylindrical hole that burrowed quickly to some (repeatable) depth and then abruptly stopped. While the jet remained, the hole maintained its steep sides and sand was being

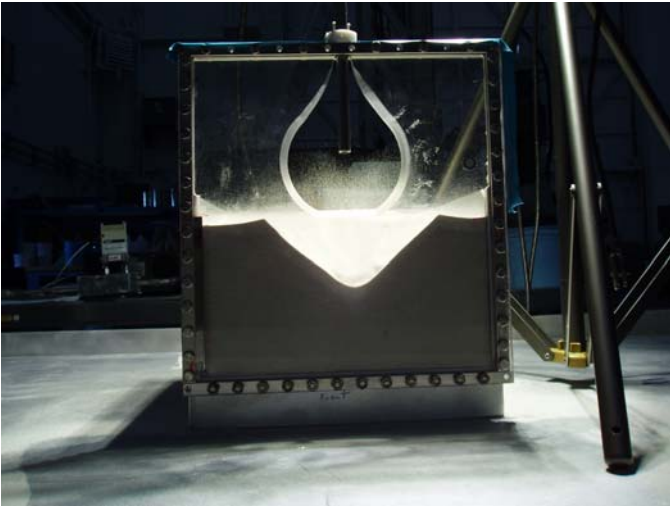


Fig. 6. Test apparatus with window at front of sandbox. The curved shape above the sand is the beveled cutout in the window, intended to reduce the interference of the window with the gas jet while yet blocking sand from falling in front of the box and thus obscuring the view.



Fig. 7. Crater formation with inner paraboloidal crater and outer conical crater.

pulled up along the sides to deform the horizontal, colored layers of sand upward along both sides of the hole. When the jet was extinguished, the narrow hole collapsed leaving only a broad, shallow crater at the surface with slopes at the angle of repose. That dynamic is why the sand appeared to be pulled upwards toward the center of the shallow crater when examining the layers of sand after the test. The hole prior to collapse was much deeper and narrower than previously recognized. The crater dimensions measured by Alexander et al [1966] were the conical, residual craters remaining at the surface and did not describe the hole prior to termination of the jet. While the jet was present, the motion of the sand exiting from the upper part of this hole may be properly characterized as turbulent aggregative fluidization [Grace and Bi, 1997]. Near the bottom of the hole no sand was entrained and growth of the hole was entirely by motion of the bulk sand beneath the surface of the crater. From the video images, we tracked individual particles in the bulk to obtain the sand's velocity field beneath its surface. The analysis is described in detail by Metzger et al [2008a]. We found that sand flows in a thick band that is tangential to the surface of the crater, dragging it away from the tip of the hole so that the hole continues growing downward, and then dragging it up the sides of the hole creating the upward deformation of sand layers described above. This flow of sand is driven by the drag force of the gas diffusing through the sand, which creates a sufficient body-force distributed throughout the sand to setup a stress state that exceeds the soil's shear strength and initiates shearing. This mechanism of sand-gas interactions had not been previously described in the literature and we are calling it *diffusion-driven shearing*, or DDS. DDS differs from BCF because the sand moves tangentially to the free surface of the crater, not perpendicularly away from the surface as predicted by the BCF mechanism. DDS differs from VE because, although both mechanisms move the particles tangentially to the surface, DDS

occurs in a thick band beneath the surface due to diffusive gas flow, whereas VE occurs only along the top layer of grains due to the free fluid flow in the boundary layer above the sand.

In the second regime of testing with slower jets of gas, the crater formed in a broad, conical shape as shown in Figure 6. With sufficient dynamic pressure of the gas the crater would also form a paraboloidal "inner" crater at the bottom of the conical crater as shown in Figure 7. The inner crater was formed by the direct action of the jet whereas the outer conical crater was the result of slope failure, avalanching sand down into the inner crater and forming the outer slope at the angle of repose. The inner crater can be understood as a transitional form of the cylindrical hole that would occur in the faster-regime of cratering, described above. Diffusion-driven shearing was observed to occur just in the very tip of the inner crater, whereas viscous erosion was the predominant mechanism throughout the remainder of the inner crater, rolling grains uphill until they reached the inner crater's lip where they went airborne. A software algorithm was developed to automatically analyze the videos frame-by-frame throughout the duration of the tests to extract crater shape and related parameters and to perform volume integrals to calculate quantities of ejected sand. The analysis was complicated by the fact that sand recirculates in the crater multiple times: the crater widens and re-ingests sand deposits that had previously fallen around its perimeter; and some of the sand falls directly back into the crater from the air. The widening crater captures and recirculates an increasing fraction of the ejected sand, and this slows down the net growth rate. Compensating for this effect, we find that the ejection of sand is actually at a constant rate throughout the test [Metzger et al, 2008a]. Furthermore, it shows that erosion rate scales linearly with the dynamic pressure of the jet ($\rho v^2/2$), which is consistent with the assumptions of Roberts' theory. In these tests, erosion occurred at the upper lip of the inner crater by VE. DDS only operated to deliver sand from the

bottom of the crater up to the sides where the gas velocity was nonzero. The grains then rolled uphill under the increasing velocity of the jet to the point where VE was occurring right at the lip of the inner crater. Similarly, in a lunar landing, DDS may occur beneath the nozzle to assist in moving the loose top layer of soil outwardly, and then grains may roll along the surface to the regions of greater shear stress where lofting finally occurs. So VE may not be the only mechanism involved in the process, but ultimately it will still be VE that controls the rate of entrainment.

A fifth type of interaction between gas and soil has also been identified, occurring only when a rocket engine is ignited over soil so that the impinging gas sends a shockwave into the soil prior to the formation of the standoff shock. This shockwave modifies the soil's compaction as it passes through, as well as possibly breaking cohesive bonds. This has been observed in recent tests with solid rocket motors firing into a meter-deep sandbox [Metzger et al, 2007]. In these tests it appears that orders-of-magnitude greater surface erosion occurs during the transient impingement of the shockwave on the sand. A similar effect occurs at the Space Shuttle launch pad when concrete is excavated and blown out from the flame trench by the impinging shock [Lane, 2004]. These shock effects did not occur in the Apollo lunar landings because the stagnation pressure on the soil developed more gradually during descent. This effect must be considered in the future if we launch spacecraft directly from the lunar surface, unlike in Apollo where the descent stage was left behind, shielding the soil.

DUST EJECTION ANGLES IN APOLLO LANDING VIDEOS

During the Apollo landings, the *descent imager camera* was a film camera mounted in the right-side window looking downward and forward from the LM. The videos show not only the cloud of blowing dust but also the shadow of the LM draped across that cloud as shown in Figure 3. From the distortion of the LM's shadow it is possible to measure the shape of the cloud and extract information about the ejection angle. To perform this analysis, we worked with a computer model of the LM developed by Sullivan [2004]. We also took physical measurements of an LM remaining from the Apollo program, located at the Kennedy Space Center. The three-dimensional measurements were accomplished using a photogrammetry system developed for the Space Shuttle Columbia investigation [Lane and Cox, 2007] in which a *photogrammetry cube* with reference markings is placed in the field of view and photographs are taken of the total scene from multiple perspectives. Software developed for this system is used to interpret the set of images three dimensionally and obtain measurements between pairs of points throughout the scene. Based on these LM dimensions, a geometric analysis of the shadows [Immer et al, 2008] indicates that the visible part of the dust cloud is usually leaving the vicinity of the LM at an ejection angle less than 3 degrees, as shown in Table 1. Several measurements were obtainable for most missions, depending on the number of usable images and the number of points where the LM altitude was audibly announced by the crew during the descent. For Apollo 12 the sun angle was too low to make measurements. For Apollo 15 the

Table 1. Dust Ejection Angles Measured from LM Shadows

Mission	Sun Angle	Ejection Angle
11	10.8	2.3
		2.3
12	5.1	-
14	10.3	2.5
		2.7
15	12.2	7.8
		7.2
		11.8
16	11.9	1.0
		1.4
		1.4
17	13.0	2.0
		1.6

dust angles were remarkable higher. Examining the landing terrain shows that the shallow crater beneath the cloud was probably responsible for this discrepancy, and in fact the high angle probably represents the real ejection angle of the dust leaving from the sloped forward bank of the crater. Since we lack a sufficient understanding of the erosion physics to model the ejection angle from first principles, we have used these empirical values for the subsequent modeling.

It should also be noted that in Apollo 15 the motion of the shadows in the final seconds of landing indicate that a "blowout" event occurred in which a high volume blast of soil was ejected at a much higher elevation angle. Unfortunately, it is impossible to measure this steeper ejection angle since the shadows are driven outside the field of view. Our best estimate, extrapolating the velocity of the shadows beyond the field of view, indicates the soil ejection angle was probably greater than 22 degrees for that brief moment. We believe that landing on a leveled and/or artificially stabilized surface may be required in the future if it is necessary to entirely eliminate these blowout events in the vicinity of the lunar outpost.

MODIFIED ROBERTS' MODEL

To estimate the quantity and trajectories of soil and dust blown at the Surveyor III spacecraft, we have modified Roberts' model in the following ways [Metzger et al, 2008b]. First, we have integrated the equations over a realistic particle size distribution of lunar soil. To obtain an analytical form for this distribution we have measured a quantity of the lunar soil simulant JSC-1A using a Sci-Tec Fine Particle Analyzer to obtain very smooth statistics of the particle count distribution as shown in Fig. 8. An exponential decay fits the JSC-1A data sufficiently over the entire range above 10 microns. It is uncertain whether JSC-1A is representative of real lunar soil below 10 microns, so we believe that this functional form is, for the present, an adequate approximation over the entire range. The limits of integration over this size distribution were obtained using Roberts'

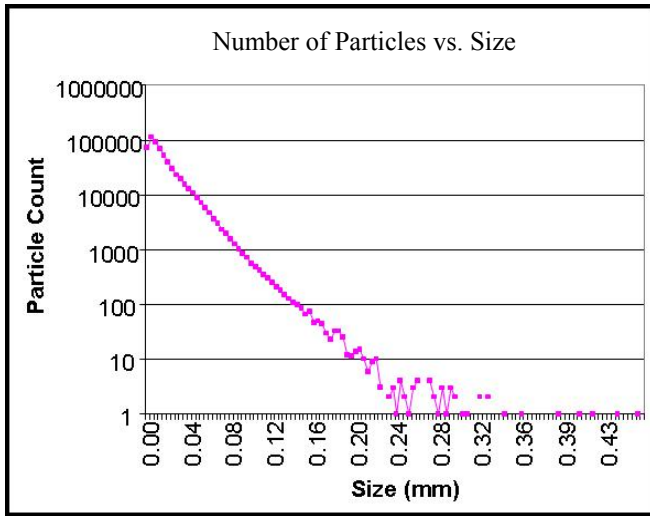


Fig. 8. Number count distribution for JSC-1A particle sizes.

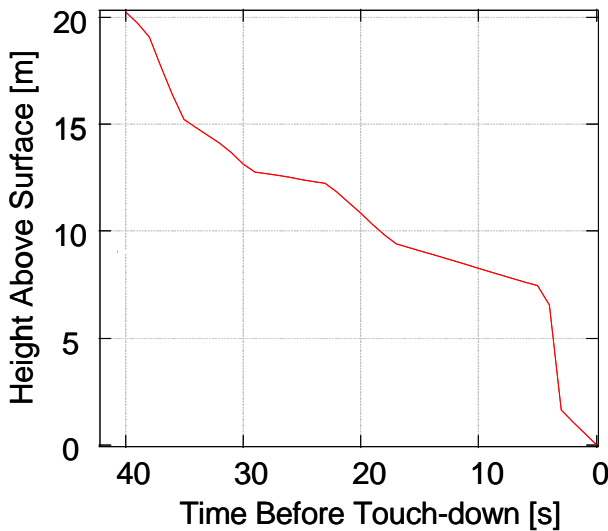


Fig. 9. Apollo 12 LM descent trajectory.

equations. This predicts that the eroded particle sizes will be between 1 μm and 1 mm, with smaller particles being inseparable due to cohesion and larger particles being inerodible due to excessive mass relative to the aerodynamic forces. We have evidence in the Apollo landing videos that much larger particles than 1 mm are actually being eroded, and we suspect that Roberts' model is incorrect in this regard because it inadequately represents the aerodynamics forces in the boundary layer along the lunar surface. Nevertheless, this will not affect the estimate of the damage to the Surveyor because such large particles are relatively few and unless a remarkably large piece of gravel were to strike the Surveyor they would represent only a minor fraction of the total damage.

Second, we have replaced Roberts' estimate of ejection angle (based on the evolving crater shape of the soil) with a narrow

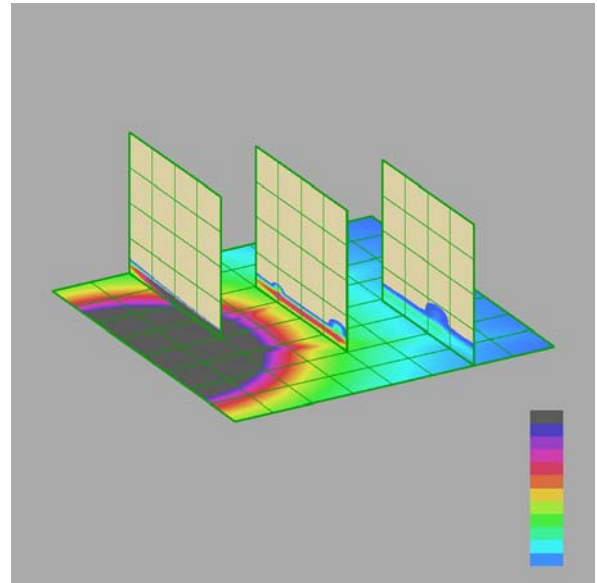


Fig. 10. Example of type of output presented by modified Roberts model, showing mass flux of blowing soil in a 3D map

distribution of angles clustered around the empirically-determined values. Third, we have integrated the resulting equations over the Apollo 12 LM descent trajectory as estimated from voice callouts of altitude by the astronauts during the landing, as shown in Fig. 9.

An example of the soil flowfield predicted by the model is shown in Fig. 10. The model predicts the velocity of the eroded particles as a function of their size and of the LM altitude, as shown in Fig. 11. The highest velocities (for the smallest particles) are close to lunar escape velocity, 2.38 km/s. For example, a 10 μm particle may be blown at 1.9 km/s when the LM is near touchdown, and at that velocity and with a 3 degree ejection angle the trajectory will be as shown in Figure 12. This range of velocities agrees with the observation of Apollo 11 mission commander Neil Armstrong that the horizon became obscured by a tan haze [Armstrong et al, 1969]. This indicates that dust had sufficient velocity that the ballistics (with our empirically-measured 3 degree ejection angle) could take it beyond the horizon. At 24 m, the altitude when dust blowing began, the ballistics require a minimum velocity of 487 m/s. This is in the range of predicted velocities for the dust. The model also predicts that there would have been 3.1 divots/cm² on the Surveyor due to the landing LM. This compares to the same order of magnitude as the estimated 1.4 divots/cm² actually observed. In fact, considering the many large sources of error in the modeling at present, it must be admitted as coincidence that the comparison came out so well. Nevertheless, we take it as evidence that the model is good to the correct order of magnitude. The model also predicts that the total volume of soil removed in the Apollo 12 landing was 787 liters, intermediate to the values of Mason (36-57 liters) and Scott (1460-2080 liters, assuming Scott had used a cylindrical crater shape). The model predicts the maximum radius of erosion to be 7.57 m. Crudely

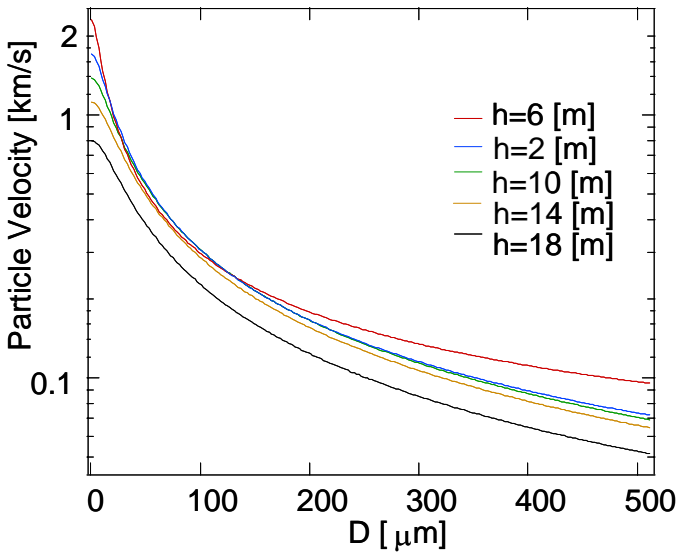


Fig. 11. Predicted particle velocities as a function of diameter for several LM altitudes.

estimating the erosion depth by assuming a conical crater shape, we predict only 1.3 cm at the center. Our model predicts a much wider erosion radius than the value used by Mason, and so despite the much larger erosion volume our predicted depth comes out comparable to the values of Mason (1.3 – 2.0 cm).

OPTICAL DENSITY IN APOLLO LANDING VIDEOS

It is also possible to measure the optical density of the dust cloud in the landing videos to extract information about the number of particles entrained in the gas. The calculation was performed by measuring the brightness of the image on a sunlit face of a rock and in its adjacent shadow, both when the dust cloud is present and when there is a momentary clearing of the cloud [Immer et al 2008]. These four data points enable a calculation of the mass density from Mie scattering,

$$\rho = \frac{-m_g}{\pi a^2 Q_{\lambda} s} \ln \frac{I_{b,2,\lambda}(\text{measured}) - I_{s,2,\lambda}(\text{measured})}{I_{b,1,\lambda}(\text{measured}) - I_{s,1,\lambda}(\text{measured})} \quad (1)$$

where ρ is the mass density of the cloud, m_g is the average mass of the dust grains, πa^2 is the average cross sectional area of the particles, s is the path-length of the light passing from the sun through the cloud to the ground and then back to the camera, Q_{λ} is the extinction coefficient of the mineral, assumed here to be unity for sufficiently large dust grains, and the four values of I_{λ} are the measured intensity of the image for the four cases, with the additional subscripts b or s representing “bright” and “shade” and 1 or 2 representing “without” or “with” the dust cloud, respectively. This calculation estimates that there are on order of 10^8 particles/ m^3 entrained in the cloud. This compares poorly with the modified Roberts’ model describe above, which predicts only 10^6 particles/ m^3 , an error of two orders of magnitude.

The underestimation of the Roberts’ model is not hard to understand. The optical density is controlled primarily by the

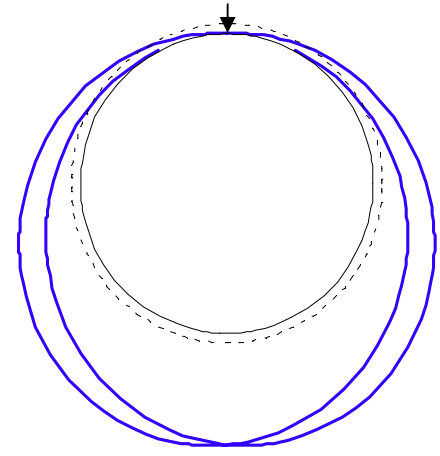


Fig. 12. (Black) Circumference of Moon. (Dashed) Altitude of orbiting Command Module, for reference. (Arrow) landing site of LM. (Blue) Trajectories of particles blown forward and backward from LM at 3 degree ejection angle and 1.9 km/s velocity.

smallest erodible particle size, because the most surface area in the cloud is due to the smallest particles, which are more numerous and have the greatest area-to-mass ratio. The cohesion of lunar soil is still one of its least understood characteristics, and so Roberts’ model made crude assumptions about the cohesive forces that would prevent the smallest particles from separating. A small error in that assumption produces a large error in optical density without greatly affecting the predicted number of divots (caused by the larger particles) or the total mass of eroded soil. In his final paper on the topic, Roberts [1964] wrote,

...there is negligible loss of visibility until the vehicle descends to this altitude [i.e., 20 feet, or 6m]; below 20 feet [6m], downward visibility may be reduced but lateral visibility will not be affected.

In contrast, the Apollo 12 mission report and crew debriefing say the following:

On Apollo 12 the landing was essentially blind for approximately the last 40 feet. [McDivitt, 1970]

...the dust went as far as I [Pete Conrad] could see in any direction and completely obliterated craters and anything else. All I knew was there was ground underneath that dust. I had no problem with the dust, determining horizontal or lateral velocities, but I couldn't tell what was underneath me. I knew I was in a generally good area and I was just going to have to bite the bullet and land, because I couldn't tell whether there was a crater down there or not....[After landing] it turned out there were more craters around there than we realized, either because we didn't look before the dust started or because the dust obscured them. [Conrad et al, 1969]

So it is not surprising that the measurement of optical density is a few orders of magnitude different than Roberts' predictions that

were made with inadequate information on the cohesive forces.

DISCUSSION

To-date, the best method for predicting the erosion rate of soil is still based on Roberts' method. Scott's calculation based on the total surface scouring of the Surveyor (rather than its divot count) assumed particles much larger than the dust fraction present in the soil, and thus overestimated the erosion rate. Mason's estimate was an order of magnitude smaller than ours and therefore does not agree well with the divot count on Surveyor III. We suggest that the use of small-scale testing in Mason's estimate may have contributed some error to the prediction. Much progress has been made in understanding granular media in the past several decades, and it is generally understood that granular phenomena are often unscalable. That is because, unlike ordinary fluids where the size of the molecules is irrelevant, the size of the sand grains is an important length-scale in the physics and so keeping all the important non-dimensional parameters constant requires the testing to be done only at full scale. For example, in the testing by Clark et al discussed above, the Knudsen number was not kept constant, although it is important in determining the drag forces on the sand and thus the erosion rate. Also, the length scale of the diffused gas pressure field (e.g., the pressure divided by its own gradient) was not addressed in the small scale tests, although it is important in DDS to determine whether the soil will shear and form a deep crater (as seen in the small scale testing but not in the Apollo landings).

Roberts' method works from first-principles, assuming that the shear stress in the gas is exactly consumed by the change in momentum of the eroding soil, so that the erosion rate self-adjusts to the shear stress. To be more accurate, future modeling will need to account for the increasing shear strength of the soil with depth due to increasing soil compaction with depth [Mitchell et al, 1974]. It should account for the physical processes directly under the nozzle that push soil out to the annular region where VE occurs, since this soil will be uncompacted in contrast to the undisturbed soil in that region. It should also improve the model of aerodynamic forces on the particles. They are not well-understood in part because the structure of the boundary layer has not been characterized well for this supersonic, highly rarefied flow, and because the lift and drag coefficients around a tiny particle under the same conditions have not been studied in detail. Furthermore, the nature of turbulence and its effects in dispersing particles upward through this boundary layer are not well-known. Finally, the role of particle collisions in dispersing the dust cloud vertically and in transferring momentum between smaller and larger particles has not been determined. Preliminary modeling has been performed with Lagrangian calculation of the individual particle trajectories decoupled from an Eulerian calculation of the gas flow field [Lane et al 2008, Lumpkin et al 2007]. The results suggest that particle dispersion by turbulence and/or particle collisions is probably important because lift and drag alone are inadequate to explain the particle dynamics observed in the landing videos. For these reasons, we cannot yet predict the erosion rate with an expectation of accuracy, and neither can we predict the ejection

angles as a function of particle size from first principles. It is quite likely that larger and smaller particles will be segregated into different ejection angles in this process (as suggested by preliminary modeling). Unfortunately, the measurement of ejection angles from the landing videos only tells us about the finest particles that have the greatest optical density. We do not know if the larger particles, say 100 microns and larger, go into a higher trajectory (as some preliminary simulations suggest). This is an important because it was the larger particles that caused the divots in the Surveyor III, while the finer particles were responsible for scrubbing permanent shadows into its finish.

Despite these uncertainties, the work to-date suggests that a berm built out of lunar soil around the landing site may be highly effective at mitigating the damage to surrounding hardware. The berm could easily be built high enough to stop a 3 degree ejection angle of fine particles, and the large particles will be going sufficiently fast that even if they fly over the berm then they should pass right over the outpost, as well. The only concern would be the largest particles, such as gravel or small rocks, which might fly with sufficiently low velocities that they could be lofted over the berm and then arc downward to strike the outpost that is behind it. Further work is required to determine the maximum size particle that can be lofted, which is still uncertain as long as the aerodynamic forces are uncertain.

In order to support future lunar operations, a physics-based numerical model is being developed to incorporate all the known mechanisms of gas-soil interactions. If the unknown aspects of the physics are sufficiently characterized, and if the model is properly coded, then it will seamlessly predict all the mechanisms that may occur for the larger and multi-engine landers that may be used in the future, as a function of the propulsion system, trajectory, and soil characteristics.

SUMMARY AND CONCLUSIONS

Our present understanding of lunar plume effects is based on a synthesis of the astronaut observations, measured Surveyor III effects, analysis of Apollo videos and photographs, terrestrial experiments, and simulations of the physics. This synthesis demonstrates rough consistency between the various sources of knowledge. Some of the older methods developed to predict this problem (some of which were not reviewed here) are not adequate because they over- or under-predict the quantity of blown soil and predict incorrect ejection angles. More work is needed to be able to predict these things entirely from first principles. Left unchecked, the spray of soil will cause unacceptable effects upon the hardware and materials in the vicinity of the lunar outpost. The particles travel at such high velocity that it is not possible to get far enough away from the spray to prevent these effects. Because of the low ejection angle for most of this spray, it seems feasible to use a berm or other physical obstruction to block most of the material.

REFERENCES

- Alexander, J. D., W. M. Roberds, and R. F. Scott [1966], “*Soil Erosion by Landing Rockets*,” Contract NAS9-4825, Hayes International Corp., Birmingham, AL.
- Alred, J. W. [1983], “Flowfield Description for the Reaction Control System of the Space Shuttle Orbiter,” AIAA-83-1548, *Proc. of AIAA 18th Thermophysics Conference*, Montreal, Quebec.
- Armstrong, N.A., M.Collins, and E.E. Aldrin [1969], “*Apollo 11 Technical Crew Debriefing*,” Vol. 1, NASA Johnson Space Center, Houston, TX, pp. 9.27 1 9.29.
- Benson, R. E., et al. [1970]. “Preliminary Results from Surveyor 3 Analysis” in *Apollo 12 Preliminary Science Report*, NASA, Washington, DC, p. 219.
- Brownlee, D., W. Bucher, and P. Hodge [1972], “Part A. Primary and secondary micrometeoroid impact rate on the lunar surface: a direct measurement,” in *Analysis of Surveyor 3 material and photographs returned by Apollo 12*, NASA, Washington, DC, pp 143-150.
- Carrier, W.D., III, G.R. Olhoeft and W. Mendell [1991], “Physical Properties of the Lunar Surface,” in *Lunar Sourcebook, A User’s Guide to the Moon* (G. H. Heiken, D.T. Vaniman and B.M. French, eds.), Cambridge University Press, Melbourne, Australia, pp. 475-594.
- Clark, L.V. and N.S. Land [1963], “Dynamic Penetration and Erosion of Dust-Like Materials in a Vacuum Environment,” *A Compilation of Recent Research Related to the Apollo Mission*, NASA Langley Research Center, Hampton, VA, pp. 145-154.
- Clark, L.V. [1970], “*Effect of Retrorocket Cant Angle on Ground Erosion – a Scaled Viking Study*,” TM X-2075, NASA Langley Research Center, Hampton, VA
- Conrad, C., R.F. Gordon, Jr., and A.L. Bean [1969], *Apollo 12 Technical Crew Debriefing*, NASA Johnson Space Center, Houston, TX, Vol. 1, pp. 9.11-9.12.
- Dohnanyi, J. S. [1966], “Remark on the Rocket Plume – Lunar Surface Erosion Problem,” TM-66-1011-2, Bellcomm, Washington, D C.
- Foreman, K. M. [1967], “*The Interaction of a Retro-Rocket Exhaust Plume with the Martian Environment*,” Grumman Res. Dept. Memorandum RM-354, Grumman Aircraft Engineering Corp., Bethpage, NY.
- Grace, J.R. And H. Bi [1997], “Introduction to circulating fluidized beds,” in *Circulating Fluidized Beds* (J.R. Grace, A.A. Avidan, and T.M. Knowlton, eds.), Blackie Academic and Professional, New York, NY.
- Hutton, R.E. [1968], “*Comparison of Soil Erosion Theory with Scaled LM Jet Erosion Tests*,” NASA-CR-66704, TRW Systems Group, Redondo Beach, CA.
- Hutton, R.E., H.J. Moore, R.F. Scott, R.W. Shorthill, and C.R. Spitzer [1980], “Surface Erosion Caused on Mars from Viking Descent Engine Plume,” *The Moon and the Planets*, Vol. 23, pp. 293-305.
- Immer, C.D., P.T. Metzger, and J.E. Lane [2008], “Apollo Video Photogrammetry Estimation of Plume Impingement Effects,” *Earth and Space 2008, 11th Biennial ASCE Aerospace Division International Conference on Engineering, Construction and Operations in Challenging Environments*, Long Beach, CA.
- Jaffe, L. D. [1972], “Part I. Blowing of Lunar Soil by Apollo 12: Surveyor 3 Evidence,” in *Analysis of Surveyor 3 material and photographs returned by Apollo 12*, SP-284, NASA, Washington DC, pp 94-96.
- Katzan, C.M. and J.L. Edwards [1991], “*Lunar Dust Transport and Potential Interactions With Power System Components*,” NASA Contractor Report 4404, Sverdrup Technology, Brook Park, OH, pp. 8-22.
- Ko, H.-Y. [1971]: “*Soil Properties Study*,” Viking Project Report VER-181, Martin Marietta Corp, Denver, CO.
- Land, N.S. and L.V. Clark [1965], “*Experimental Investigation of Jet Impingement on Surfaces of Fine Particles in a Vacuum Environment*,” TN-D-2633, NASA Langley Research Center, Hampton, VA.
- Land, N.S. and W. Conner [1967]. “Laboratory Simulation of Lunar Surface Erosion by Rockets,” *Institute of Environmental Sciences 13th Annual Technical Meeting Proceedings*, Vol. 1, Washington, DC.
- Land, N.S., and H.F. Scholl [1966], “*Scaled Lunar Module Jet Erosion Experiments*,” TN-D-5051, NASA Langley Research Center, Hampton, VA.
- Lane, J.E. [2004], “*Ground Camera Photogrammetry 3D Debris Trajectory Analysis*,” ASRC Aerospace, Kennedy Space Center, FL.
- Lane, J.E. and R.B. Cox [2007], “*Digital Image Inspection for Spacecraft Processing*,” ASRC Aerospace, Kennedy Space Center, FL.
- Lane, J.E., P.T. Metzger, and C.D. Immer [2008], “Lagrangian trajectory modeling of lunar dust particles,” *Earth and Space 2008, 11th Biennial ASCE Aerospace Division International Conference on Engineering, Construction and Operations in Challenging Environments*, Long Beach, CA.
- Lumpkin, F., J. Marichalar, A. Piplica (2007), “Plume Impingement to the Lunar Surface: A Challenging Problem for

DSMC,” in *Direct Simulation Monte Carlo Theory, Methods & Applications*, Santa Fe, NM.

Mason, C.C. [1970], “Comparison of Actual versus Predicted Lunar Surface Erosion Caused by Apollo 11 Descent Engine,” *Geological Society of America Bulletin*, Vol. 81, pp. 1807-1812.

Mason, C.C. and E.F. Nordmeyer [1969], “An empirically derived erosion law and its application to lunar module landing,” *Geological Society of America Bulletin*, Vol. 80, pp. 1783-1788.

McDivitt, J.A., et al [1970], “*Apollo 12 Mission Report*”, MSC-01855, NASA Johnson Space Center, Houston, TX, sect. 6.1.3.

McDivitt, J.A., et al [1971], “*Apollo 15 Mission Report*”, MSC-05161, NASA Johnson Space Center, Houston, TX, pp. 62-63.

Metzger, P.T., B.T. Vu, D.E. Taylor, M.J. Kromann, M. Fuchs, B. Yurko, A. Dokos, C.D. Immer, J.E. Lane, M.B. Dunkel, C.M. Donahue, and R.C. Latta, III, [2007], “Cratering of Soil by Impinging Jets of Gas, with Application to Landing Rockets on Planetary Surfaces,” *Proceedings of the 18th Engineering Mechanics Division Conference*, Blacksburg, VA.

Metzger, P.T., C.D. Immer, C.M. Donahue, B.T. Vu, R.C. Latta, III, M. Deyo-Svendsen, [2008a], “Jet-induced cratering of a granular surface with application to lunar spaceports,” *J. Aerospace Engineering* (accepted for publication).

Metzger, P.T., J.E. Lane, and C.D. Immer [2008b], “Modification of Roberts’ theory for rocket exhaust plumes eroding lunar soil,” *Earth and Space 2008, 11th Biennial ASCE Aerospace Division International Conference on Engineering, Construction and Operations in Challenging Environments*, Long Beach, CA.

Mitchell, J.K., L.G. Bromwell, W.D. Carrier, III, N.C. Costes, W.N. Houston, R. F. Scott, H.J. Hovland [1972a], “Soil mechanics experiment”, in *Apollo 15 Preliminary Science Report*, NASA Johnson Space Center, Houston, TX.

Mitchell, J.K., W.D. Carrier, III, W.N. Houston, R. F. Scott, L.G. Bromwell, H.T. Durgunoglu, H.J. Hovland, D.D. Treadwell, and N.C. Costes [1972b], “Soil mechanics experiment”, in *Apollo 16 Preliminary Science Report*, NASA Johnson Space Center, Houston, TX.

Mitchell, J.K., W.D. Carrier, III, N.C. Costes, W.N. Houston, R. F. Scott, H.J. Hovland [1973], “Soil mechanics; characteristics of lunar soil from Apollo 17 flight lunar landing site”, in *Apollo 17 Preliminary Science Report*, NASA Johnson Space Center, Houston, TX.

Mitchell, J.K., W.N. Houston, W.D. Carrier, III, N.C. Costes [1974], “*Apollo Soil Mechanics Experiment S-200*,” NASA contract NAS9-11266, Space Sciences Laboratory Series 15, No. 7, University of California, Berkeley, CA.

Phillips, P.G., et al [1988], “*Lunar Base Launch and Landing Facility Conceptual Design*,” NASA contract NAS9-17878, EEI Report 88-178, Eagle Engineering, Webster, TX.

Phillips, P.G., Charles H. Simonds, and William R Stump [1992], “Lunar Base Launch and Landing Facilities Conceptual Design,” in *The Second Conference on Lunar Bases and Space Activities of the 21st Century* (W.W. Mendell, ed.), NASA Johnson Space Center, Houston, TX, Vol. 1, pp. 139-151.

Roberts, L. [1963a], “The Action of a Hypersonic Jet on a Dust Layer,” IAS Paper No. 63-50, *Institute of Aerospace Sciences 31st Annual Meeting*, New York, NY.

Roberts, L. [1963b], “Visibility and Dust Erosion During the Lunar Landing,” in *A Compilation of Recent Research Related to the Apollo Mission*, NASA Langley Research Center, Hampton, VA, pp. 155-170.

Roberts, L. [1964], “Exhaust Jet – Dust Layer Interaction During a Lunar Landing,” *XIIIth International Astronautical Congress Varna 1962 Proceedings*, Springer-Verlag, New York, NY, pp. 21-37.

Roberts, L. [1966], “The Interaction of a Rocket Exhaust with the Lunar Surface,” in *The Fluid Dynamic Aspects of Space Flight*, Gordon and Breach Science Publishers, New York, NY, Vol. 2, pp. 269-290.

Romine, G.L., T.D. Reisert, and J. Gliozzi [1973]. “*Site Alteration Effects from Rocket Exhaust Impingement During a Simulated Viking Mars Landing. Part I – Nozzle Development and Physical Site Alteration*,” NASA CR-2252, Martin Marietta Corporation, Denver CO.

Schmalzer, P.A., S.R. Boyle, P. Hall, D.M. Oddy, M.A. Hensley, E.D. Stolen, and B.W. Duncan [1998], “*Monitoring Direct Effects of Delta, Atlas, and Titan Launches from Cape Canaveral Air Station*,” NASA TM-1998-207912.

Scott, R.F. [1975], “*Apollo Program Soil Mechanics Experiment: Final Report*”, NASA CR-1444335, California Institute of Technology, Pasadena, CA.

Scott, R.F., and H.-Y. Ko [1968], “Transient Rocket-Engine Gas Flow in Soil,” *AIAA Journal*, Vol. 6, No. 2, pp. 258-264.

Sullivan, S. P. [2004]. *Virtual LM : a pictorial essay of the engineering and construction of the Apollo lunar module, the historic spacecraft that landed man on the moon*. Apogee Books, Burlington, Ontario.

